PROCEEDINGS OF SCIENCE

Exclusive single pion electroproduction off the proton in the high-lying resonances at $Q^2 < 5$ GeV^2 from CLAS.

Kijun Park*
Old Dominion University,
4600 Elkhorn Ave.
Norfolk, VA 23529
E-mail: parkkj@jlab.org

The differential cross sections and structure functions for the exclusive electroproduction process $ep \to e'n\pi^+$ were measured in the range of the invariant mass for the $n\pi^+$ system 1.6 GeV $\leq$ W $\leq$ 2.0 GeV, and the photon virtuality 1.8 GeV^2 $\leq$ Q^2 $\leq$ 4.0 GeV^2 using CLAS at Jefferson Lab. For the first time, these kinematics are probed in the exclusive π^+ production from the protons with nearly full coverage in the azimuthal and polar angles of the $n\pi^+$ center-of-mass system. In this analysis, approximately 39,000 differential cross-section data points in terms of W, Q^2, $\cos\theta^*_\pi$, and ϕ^*_π, were obtained. The preliminary differential cross section and structure function analyses are carried out, which allow us to extract the helicity amplitudes in high-lying resonances.

XV International Conference on Hadron Spectroscopy-Hadron 2013
4-8 November 2013
Nara, Japan

*Speaker.

PoS(Hadron 2013)113

1. Introduction

The structure of the nucleon and its excited states have been one of the most extensively investigated subjects in nuclear and particle physics for several decades, because it allows us to understand important aspects of the underlying theory of the strong interactions. Many different reactions can be used to study the properties of the nucleon and its excited states. One can study the ground state nucleon using elastic scattering of eletrons off protons and neutrons in order to obtain the electric and magnetic charge distributions. The exclusive meson electroproduction off protons is a powerful tool to probe the effective degrees of freedom in excited nucleon states at different distance scales where the transition from the contributions of both quark core and meson-baryon cloud to the quark core dominance takes place.

During the last decade, several low-lying nucleon resonance states ($W < 1.6$ GeV), such as $\Delta(1230)3/2^+$, $N(1440)1/2^+$, $N(1520)3/2^-$, and $N(1535)1/2^-$ [1, 2, 3] have been studied to help our understanding of new insights into nucleon structure. However, the $SU(6)$x$O(3)$ scheme still predicts many well-known resonances with four star rating in the high mass region. There is also a big gap between the dressed quark regime and the perturbative QCD domain. In order to establish a better understanding of the connection between the two regimes at high Q^2, it is important to measure fundamental observables, such as cross sections or asymmetries for the excited resonance region. The various current resonance models predict not only a different excitation spectra but also different Q^2 dependence of the transition form factors. For example, the light cone sum rule (LCSR) has been used to predict recently the Q^2 evolution of the $N(1535)1/2^-$ resonance for both the transverse ($A_{1/2}$) and longitudinal ($S_{1/2}$) helicity amplitudes [4]. The mapping of the transition form factors for high-lying resonances will help us to better understand the underlying quark or hadronic structures [5]. With new data on meson electroproduction, combined with the large coverage in Q^2, W, and center-of-mass angles, the study of nucleon resonances will become even more powerful tool in the exploration of nucleon structure in the domain of strong QCD and confinement.

In this proceeding, preliminary differential cross sections and structure functions for $p(e,e'\pi^+)n$ are presented in the high invariant mass region, $W = 1.6-2.0$ GeV, for $Q^2 = 1.8-4.0$ GeV^2. This measurement has been performed by utilizing the CLAS in Hall-B at Jefferson Lab. CLAS is a large acceptance instrument with sufficient resolution to measure the exclusive electroproduction of mesons with nearly complete coverage in the center-of-mass angles, which allows for a detailed study of the excitation of nucleon resonances. The measurement of the differential cross sections in the high W, Q^2 kinematic regions allows us to extract helicity amplitudes for the high-lying resonance states, such as $N(1680)F_{15}$, $N(1675)D_{15}$, $N(1710)P_{11}$.

2. Results

We analyze a set of events in which an electron beam incident upon a hydrogen target produced a final state consisting of the scattered electron and one baryon and one meson. Specifically, we analyzed the $e1f$ data set which was taken in the spring of 2003 for events of a type ^{1}H$(e,e'\pi^+)n$ where we detected the scattered electron and one positively charged particle (a π^+) and determined by a missing mass technique that the undetected neutral particle was a neutron. These experimental

conditions entailed an electron beam of energy 5.5 GeV, with a typical current of 7 nA, incident on a 5 cm long hydrogen target. The particle identification and kinematic corrections are applied for the entire kinematic region. The CLAS electron identification at the trigger level is done by requiring a minimum amount of energy in the electromagnetic calorimeter in coincidence with a signal in the Cherenkov counter. Pions are identified by a coincidence of drift chamber and time-of-flight counter. A kinematic correction and proper geometrical fiducial cuts are applied to both simulation and experimental data. The fiducial cuts are to select areas of uniform detector response that can be reproduced by the GEANT Simulation [6]. For each event, the missing mass recoiling from the scattered electron and identified pion was calculated and, by accumulating over all events, a missing mass distribution was formed for each bin. The single charged pion electroproduction cross section factorizes in Eq. (2.1) under the one-photon-exchange approximation.

$$\frac{k^*_\gamma}{p^*_\pi}\frac{d^2\sigma}{d\Omega} = \sigma_T + \varepsilon\sigma_L + \varepsilon\sigma_{TT}\sin^2\theta^*_\pi\cos 2\phi^*_\pi + \sqrt{2\varepsilon(1+\varepsilon)}\sigma_{LT}\sin\theta^*_\pi\cos\phi^*_\pi\,, \tag{2.1}$$

where p^*_π, θ^*_π are the π^+ momentum and polar angle in the center-of-mass frame. ϕ^*_π is the azimuthal rotation of the $n\pi^+$ plane with respect to the electron scattering plane (e,e'), k^*_γ is the equivalent photon energy, and ε is the virtual photon polarization.

Our choice of bin sizes represents a trade-off between the better statistics resulting from a choice of fewer, and larger, bins and the several advantages offered by smaller bins. One advantage of the latter is to have better granularity in determining the dependence of the cross sections on the variable in question; for example, we chose moderately fine bins in W (10 MeV) in order to evaluate the influence of various baryonic resonances but we chose only 12 bins in ϕ^*_π because of reduced statistics. Similarly, we chose alternative bin-size in ϕ^*_π (for example 24 or 48) with coarse W (40 or 60 MeV) bin-size in order to see the consistency in cross sections [7].

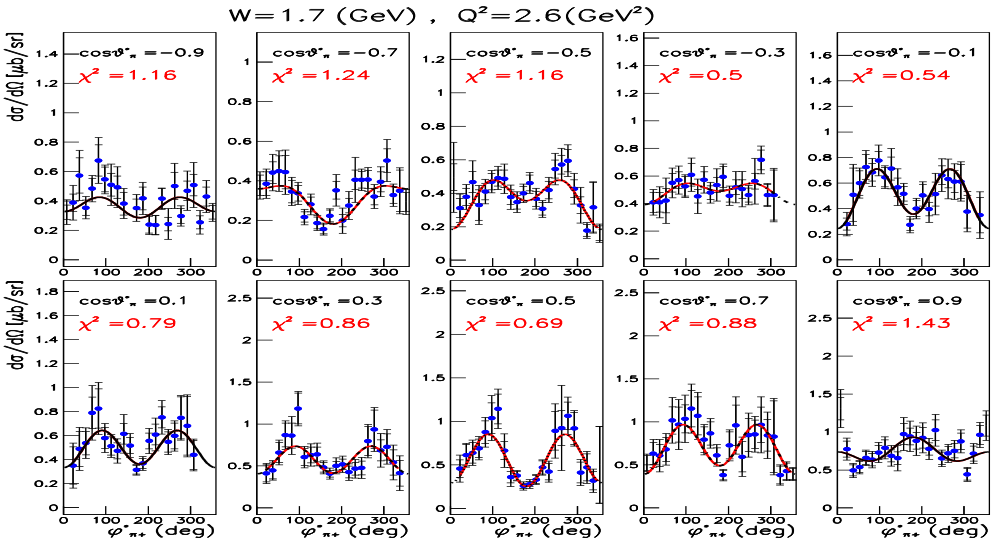

Figure 1: (Color online) Examples of the preliminary $d\sigma/d\Omega$ and fit at $W = 1.7$ GeV, $Q^2 = 2.6$ GeV^2. The outer error-bars show the systematic uncertainties. Curves are fits with Eq. (2.1).

Figure 1 shows examples of preliminary cross sections as a function of ϕ_π^* and fit at $W = 1.7$ GeV, $Q^2 = 2.6$ GeV^2. The fit of ϕ_π^*-dependent cross sections allows us to obtain the structure functions. The fit is done taking total uncertainty into account by adding statistical and systematic uncertainties in quadrature. The overall systematic uncertainty is approximately $8\% - 10\%$. The fit function has three parameters, $d\sigma/d\Omega = P_1 + P_2 \cos\phi_\pi^* + P_3 \cos 2\phi_\pi^*$, which correspond to the structure functions $P_1 = \sigma_T + \varepsilon\sigma_L$, $P_2 = \sigma_{LT}$ and $P_3 = \sigma_{TT}$, respectively.

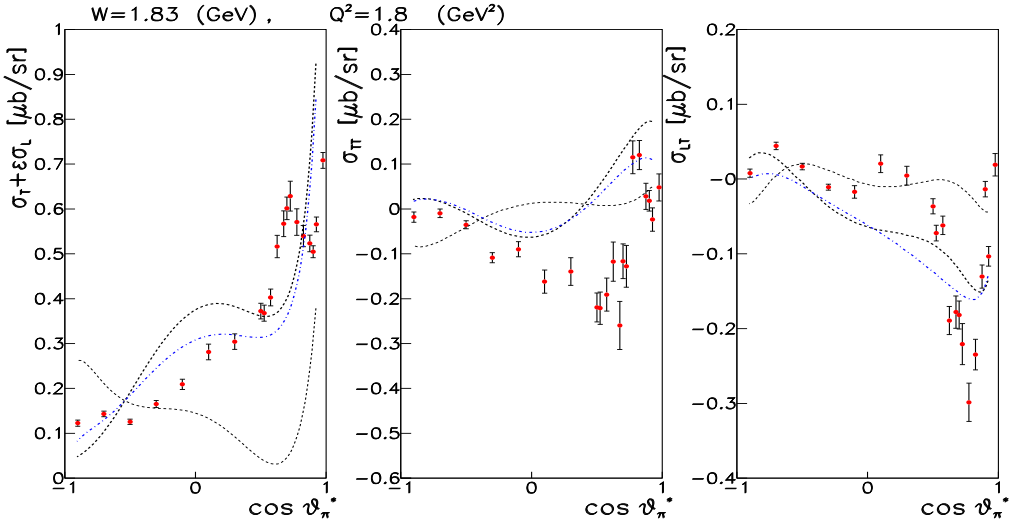

Figure 2: (Color online) An example of the structure functions ($\sigma_T + \varepsilon\sigma_L$, σ_{TT}, and σ_{LT}) as a function of $\cos\theta_\pi^*$ at $W = 1.83$ GeV, $Q^2 = 1.8$ GeV^2. Curves are DMT (thin dashed), MAID2003 (dash-dotted), and MAID2007 (bold dashed) models.

Figure 2 shows three structure functions as a function of $\cos\theta_\pi^*$ at $W = 1.83$ GeV, $Q^2 = 1.8$ GeV^2 and existing physics models. Presently, few physics models are available such as Dubna-Mainz-Taipei (DMT) [8], MAID2003 [9], and MAID2007 [10], which are thin dashed, dash-dotted, and bold dashed lines, respectively. However, most of existing physics models do not support any of the results to high W. Fitting our differential cross sections, we extracted amplitudes from the averaged values of the results obtained using the Unitary Isobar Model (UIM) [10] and Dispersion Relations (DR) [11, 12]. The uncertainty that originates from the averaging is considered as one of the model uncertainties. Since the UIM and DR analyses give fits of the same overall quality we assign the difference between the two results as one component of the model uncertainty. Following the analysis made in Ref. [12], we consider also two other kinds of model uncertainties: (1) the uncertainties of the background of UIM and the Born term in DR, (2) the uncertainties of the widths and masses of the resonances. All these uncertainties where studied and added in quadrature.

At the values of Q^2, the resonance $N(1680)F_{15}$ together with the pairs of the resonances $\Delta(1620)S_{31}$, $N(1650)S_{11}$ and $\Delta(1600)P_{33}$, $N(1720)P_{13}$ are responsible for about 80% of all resonance contribution to the $\gamma^* p \to n\pi^+$ total cross sections in the third resonance region. Each of them accounts for about one third of this contribution, which is demonstrated in Figure 3. It shows on the $N(1680)F_{15}$ contribution to other moments as well as the Legendre moments from the fit to the experimental cross sections.

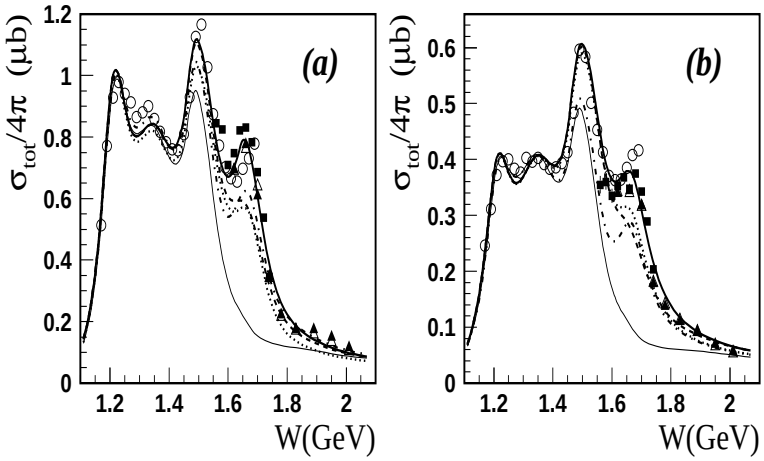

Figure 3: The $\gamma^* p \to n\pi^+$ total cross sections ($\sigma_{tot}/4\pi = D_0^{T+L}$) at $Q^2 = 1.8$ GeV^2 (a) and 3.15 GeV^2 (b). Open circles are [6] and solid symbols from this work. The thick solid curves correspond to the results obtained using UIM. The dashed, dotted, and dashed-dotted curves are obtained, respectively, by switching off the contributions of $N(1680)F_{15}$, ($\Delta(1620)S_{31}$ and $N(1650)S_{11}$), and ($\Delta(1600)P_{33}$ and $N(1720)P_{13}$) from the UIM results. The thin solid curves are obtained by switching off all resonance contributions from the third resonance region.

3. Acknowledgment

We would like to acknowledge the outstanding efforts of the staff of the Accelerator and the Physics Divisions at JLab that made this experiment possible. The Southeastern Universities Research Association (SURA) operated Jefferson Lab under United States DOE contract DE-AC05-84ER40150 during this work.

References

[1] I.G. Aznauryan, V.D. Burkert, *et al.*, Phys. Rev. C 71, 015201; Phys. Rev. C 72, 045201, (2005).

[2] I.G. Aznauryan, V.D. Burkert, K. Park, *et al.*, Phys.Rev.C 78, 045209 (2008).

[3] I.G. Aznauryan, Phys. Rev. C 76, 025212, (2007).

[4] V.M. Braun, D.Yu. Ivanov, A. Lenz and A. Peters, Phys. Rev. D 75, 014021 (2007).

[5] V.D. Burkert and T.-S. H. Lee, Int. J. Phys. E 13, 1035, (2004).

[6] K. Park *et al.*, Phys. Rev. C 77, 015208, (2008).

[7] K. Park, V.D. Burkert, I.G. Aznauryan, An internal CLAS analysis note (2014).

[8] S.S. Kamalov and S.N. Yang, *et al.*, Phys. Rev. Lett. 83, 4494 (1999).

[9] D. Drechsel, O. Hanstein, S. Kamalov, and L. Tiator, Nucl. Phys. A 645,145-174,(1999).

[10] D. Drechsel, S.S. Kamalov, and L. Tiator, Eur. Phys. J. A 34, 69 (2007).

[11] I.G. Aznauryan, Phys. Rev. C 67, 015209 (2003).

[12] I.G. Aznauryan, V.D. Burkert, K. Park, *et al.*, Phys. Rev. C 80, 055203 (2009).